JOURNAL OF THE FACULTY OF ENGINEERING, THE UNIVERSITY OF TOKYO (B)
Vol. XXXVII, No. 3 (1984)

J-Integral Method in Analysis of Stress Intensity Factor Using Boundary Elements

by
Koichi KISHITANI*, Takayuki HIRAI** and Kiyoshi MURAKAMI*

(Received September 28, 1983)

Remarkable progress has recently been made regarding studies of the Boundary Element Method. It has been reported in many papers that BEM offers a powerful means of calculating numerical solutions of engineering problems. Elastic analysis of crack propagation is one of the problems, and in such case BEM is superior in accuracy and economy compared with domain type methods such as the Finite Element Method and the Finite Differential Method.

There are two different methods of formulating BEM, the direct and indirect methods. For development of a BEM program which can be utilized for an arbitrary boundary value problem, formulation of the indirect method is superior to formulation of the direct method with respect to accuracy of numerical solutions.

A crack analysis technique using BEM based on formulation of the indirect method is developed, and the effectiveness of the present method is shown for a number of examples of analyses concerning crack problems with arbitrary boundary conditions.

1. Introduction

The stress intensity factor is a useful criterion of crack propagation in linear fracture mechanics, and in structural engineering is used for discribing failures of brittle materials. Accurately evaluating the stress intensity factor of cracks of arbitrary geometrical conditions in practical problems is a matter of great importance. It is looked forward to that BEM will be a potent analysis weapon in this case.

BEM is a boundary type method which has recently drawn attention. Compared with domain type methods such as FEM and FDM, BEM possesses the following prominent features: input data are simple since the number of dimensions of space to be the object of discretion is reduced by one, and the accuracies of solutions, especially the stress concentration solution, are good since a fundamental solution rigidly satisfying the governing equation of elasticity is used.

The path independent integral (called J-integral) introduced by Rice[7], is generally of better accuracy than other techniques and is recognized as being economical. J-integral is a line integral along an arbitrary path surrounding a crack tip inside the domain. Since BEM has a solution of very good accuracy inside the domain, it is thought that the J-integral method using it will give an even more satisfactory result.

* Department of Architecture
** Department of Architecture, Ohita University

The direct and indirect methods of BEM were formulated in the preliminary studies. A two-dimensional linear elastic J-integral program was set up using BEM based on the indirect method. The present method was applied to a number of typical crack problems, and the effectiveness of the method was discussed.

2. Preliminary Study

A two-dimensional homogeneous isotropic linear elastic body having a boundary S and a domain V is considered. The notations σ_{ij}, e_{ij}, T_i, u_i and C_{ijmn} respectively stand for stress, strain, traction, displacement and elastic constants. The subscript indicates a coordinate axis, and is assumed to follow the summation convention. The meaning of the superscript is:

source → ○—□—○ ← observation

2.1 Direct Method

Differentiating fundamental solutions by the superscript *, the following well-known integral equation is obtained for the boundary value problem. However, body force is not considered.

$$\int_V {}^*\sigma_{ij,j} \cdot u_i \, dV = \int_S ({}^*T_i \cdot u_i - {}^*u_i \cdot T_i) \, dS, \tag{1}$$

When a source of the fundamental solution is not located inside the domain V, then ${}^*\sigma_{ij,j}=0$, so that Eq. (1) will become the following.

$$\int_{S_1} {}^*T_i \cdot u_i \, dS_2 - \int_{S_1} {}^*u_i \cdot T_i \, dS_1 =$$

$$- \int_{S_1} {}^*T_i \cdot u_i \, dS_1 + \int_{S_2} {}^*u_i \cdot T_i \, dS_2, \tag{2}$$

where, S_1, S_2 and the underlined values indicate the essential boundary, the natural boundary and known boundary values, respectively.

When a l-directional unit concentrated force acts at point k inside the domain, since $\sigma_{lj,j}=-1$ at point k, Eq. (1) will become;

$$u_l^k = \int_S ({}^{*kl}u_i \cdot T_i - {}^{*kl}T_i \cdot u_i) dS, \tag{3}$$

Substituting Eq. (3) in $\sigma_{ij}=C_{ijmn}\frac{1}{2}(u_{m,n}+u_{n,m})$, the stress at point k is obtained. As one example, if σ_x were to be indicated by plane stress condition,

$$\sigma_x^k = \frac{E}{1-\nu^2}\left[\int_S \left\{\frac{\partial}{\partial x}({}^{*kx}u_i) + \nu \frac{\partial}{\partial y}({}^{*ky}u_i)\right\} T_i \, dS \right.$$

$$\left. - \int_S \left\{\frac{\partial}{\partial x}({}^{*kx}T_i) + \nu \frac{\partial}{\partial y}({}^{*ky}T_i)\right\} u_i \, dS \right], \tag{4}$$

Eqs. (2), (3) and (4) are expressions which comprise the basis of the direct method for calculating boundary values, displacements and stresses within the domain, respectively.

There are two important factors which cause errors to be produced in solutions by the direct method. The first factor consists of differences between simulated boundary values and theoretical boundary values of the problem. To correct this situation, high-order boundary elements can be used, or the number of boundary elements can be increased. The authors selected the latter method and used straight segment boundary elements where boundary values are readily distributed. As shown in Fig. 1, tractions distributed linearly and displacements showing a quadratic distribution were adopted.

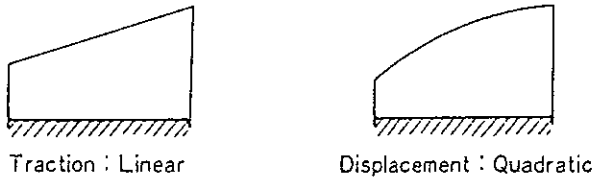

Fig. 1 Tractions distributed linearly and displacements showing a quadratic distribution adopted in the direct method

The second factor is numerical boundary integration. As methods of reducing errors in solutions an analytical formula of boundary integration and regular boundary integral equations by Patterson and Sheikh[6] can be usilized. Regarding elements including singular points of the fundamental solution, boundary integration has been analytically deduced by Brebbia[1], while numerical calculations can be performed with regard to others. Table 1 shows the results of comparison studies concerning the methods of boundary integral calculation. When boundary

Table 1. Comparisons of methods of boundary integral calculation

Problems	Without Singularity (continuous boundary condition)		With Singularity (discontinuous boundary condition)	
Boundary Integration	Numerical	Analytical	Numerical	Analytical
Singular	X	O	X	O
Regular	O	O	X	X

O sufficient X insufficient

integrations are numerically calculated, the regular boundary integral method is useful. However, when an analytical formula is used, the singular boundary integral method is superior to the regular boundary integral method. Therefore, in the analyses here, the singular boundary integral method using the analytical formula by Hirai[2] was used.

2.2 *Indirect Method*

An exterior domain enclosing an interior domain and possessing in common a boundary S is considered. It is assumed that T expresses the traction of the interior domain, and a traction $\bar{T}$ of the exterior domain acts causing a displacement u to be produced on the boundary S the same as in the interior domain. When a l-directional unit concentrated force acts on point k located inside the interior domain, the following two boundary integral equations are obtained.

$$\textit{Interior:} \qquad u_l^k = \int_S ({}^{*kl}u_t^s \cdot T_t^s - {}^{*kl}T_t^s \cdot u_t^s)\, dS, \tag{5}$$

$$\textit{Exterior:} \qquad 0 = \int_S ({}^{*kl}u_t^s \cdot \bar{T}_t^s - \underset{\sim}{{}^{*kl}T_t^s} \cdot u_t^s)\, dS, \tag{6}$$

where, a value on the boundary is shown by the superscript s.

Since the interior and exterior domains are located at opposite sides of the boundary S, $\underset{\sim}{{}^{*kl}T_t^s} = -{}^{*kl}T_t^s$.

Thereupon, from Eqs. (5) and (6), the following equation is obtained.

$$u_l^k = \int_S {}^{*kl}u_t^s (T_t^s + \bar{T}_t^s)\, dS, \tag{7}$$

If Eq. (7) is substituted in $\sigma_{ij} = C_{ijmn} \frac{1}{2}(u_{m,n} + u_{n,m})$, then ${}^{*kl}u_l^s = {}^{*kt}u_l^s$, hence the following equation is obtained.

$$\sigma_{ij}^k = \int_S (-{}^{*kt}\sigma_{ij}^s)(T_t^s + \bar{T}_t^s)\, dS, \tag{8}$$

Eqs. (7) and (8) are expressions to comprise the foundation of the indirect method.

Since ${}^{*kl}u_t^s = {}^{*st}u_l^k$ and $-{}^{*kt}\sigma_{ij}^s = {}^{*st}\sigma_{ij}^k$, if $(T_t^s + \bar{T}_t^s)$ is replaced by W_t^s, the following equation is obtained from Eqs. (7) and (8).

$$\begin{aligned} u^k &= \int_S {}^{*st}u^k \cdot W_t^s\, dS, \\ \sigma_{ij}^k &= \int_S {}^{*st}\sigma_{ij}^k \cdot W_t^s\, dS, \end{aligned} \tag{9}$$

Eq. (9) signifies that the indirect method is numerically equivalent to the superposition method. The indirect and superposition methods have been discussed in detail by Hirai[3),4)].

The solution of an elastic problem is obtained by superposition of a certain number of domains in static equilibrium in a manner that given boundary conditions will be reproduced. The static equilibrium used in superposition is calculated by the fundamental solution including the domain of the problem. At such time, the unknown quantity W signifies the size of the load system in static equilibrium producing the fundamental solution. Development of the numerical formulation of the superposition method is simpler than that of the indirect method. Hence, the formulation of the indirect method is handled below in the sense of the principle of superposition.

Figure 2 shows the kind of fundamental solution used in the indirect method. The individual fundamental solutions are derived analytically. The boundary conditions were reproduced

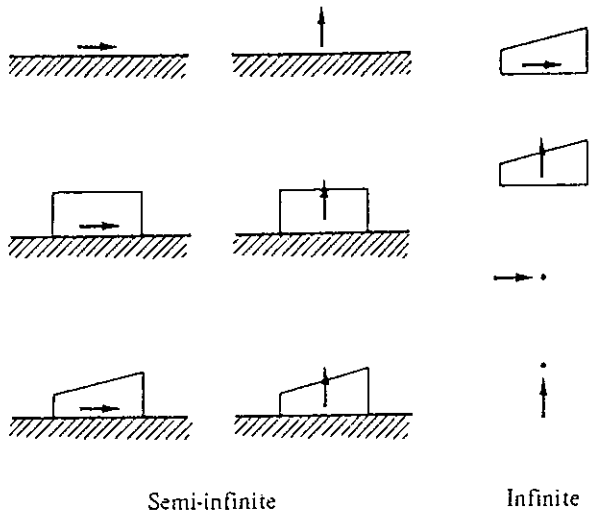

Fig. 2 Kind of fundamental solution used in the indirect method

so that through superpositioning of domains the resultant forces and moments would be equal to the conditions given on the individual elements.

2.3 Fundamental Solution

In the following, the stress and displacement field produced by linear distributed load acting in the plane of an infinite plate are shown by a plane stress condition.

Figure 3 shows the geometry of the state of load distribution, and if an orthogonal coordinate system is provided, where an element direction with the subject on the right is taken as the the positive direction of the X axis, then

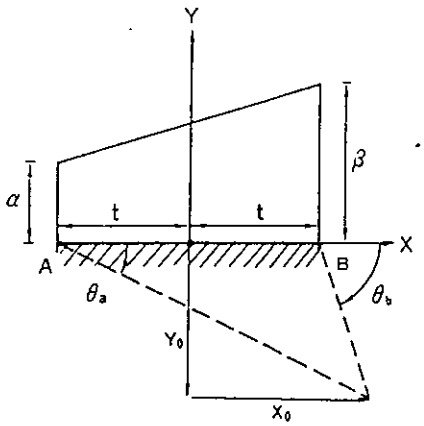

Fig. 3 Geometry of the state of load distribution

X-directional linear distributed load

$Y_0=0$

$$\sigma_x = [(m\cdot TT+\frac{3m-n}{2}\cdot FF+\frac{m-n}{4}\cdot SS)\frac{Y_0}{2t}+(m\cdot AA+\frac{m-n}{4}\cdot CC)\frac{X_0-t}{2t}]\alpha$$
$$+[-(m\cdot TT+\frac{3m-n}{2}\cdot FF+\frac{m-n}{4}\cdot SS)\frac{Y_0}{2t}-(m\cdot AA+\frac{m-n}{4}\cdot CC)\frac{X_0+t}{2t}]\beta,$$

$$\sigma_y = [-(n\cdot TT+\frac{m+n}{2}\cdot FF+\frac{m-n}{4}\cdot SS)\frac{Y_0}{2t}-(n\cdot AA+\frac{m-n}{4}\cdot CC)\frac{X_0-t}{2t}]\alpha$$
$$+[(n\cdot TT+\frac{m+n}{2}\cdot FF+\frac{m-n}{4}\cdot SS)\frac{Y_0}{2t}+(n\cdot AA+\frac{m-n}{4}\cdot CC)\frac{X_0+t}{2t}]\beta,$$

$$\tau_{xy} = [-(m\cdot AA+\frac{m-n}{4}\cdot CC)\frac{Y_0}{2t}+(\frac{m+n}{2}\cdot FF+\frac{m-n}{4}\cdot SS)\frac{X_0-t}{2t}]\alpha$$
$$+[(m\cdot AA+\frac{m-n}{4}\cdot CC)\frac{Y_0}{2t}-(\frac{m+n}{2}\cdot FF+\frac{m-n}{4}\cdot SS)\frac{X_0+t}{2t}]\beta,$$

$$u_x = [(\frac{A}{2}\cdot GG+\frac{A-2B}{4}\cdot HH-B\cdot AA)Y_0-\{A\cdot EE+(A-B)(TT+FF)\}(X_0-t)]\frac{Y_0}{2t}\cdot\alpha$$
$$+[-(\frac{A}{2}\cdot GG+\frac{A-2B}{4}\cdot HH-B\cdot AA)Y_0+\{A\cdot EE+(A-B)(TT+FF)\}(X_0+t)]\frac{Y_0}{2t}\cdot\beta,$$

$$u_y = [-(TT+FF)Y_0-AA(X_0-t)]B\cdot\frac{Y_0}{2t}\cdot\alpha$$
$$+[(TT+FF)Y_0+AA(X_0+t)]B\cdot\frac{Y_0}{2t}\cdot\beta,$$

$Y_0=0,\ |X_0|\neq t$

$$\sigma_x = -m(1+BB\cdot\frac{X_0-t}{2t})\alpha+m(1+BB\cdot\frac{X_0+t}{2t})\beta,$$

$$\sigma_y = n(1+BB\cdot\frac{X_0-t}{2t})\alpha-n(1+BB\cdot\frac{X_0+t}{2t})\beta,$$

$$\tau_{xy} = \begin{cases} 0 & (|X_0|>t), \\ -\frac{X_0-t}{4t}\cdot\alpha+\frac{X_0+t}{4t}\cdot\beta & (|X_0|<t), \end{cases}$$

$$u_x = [-\{\frac{A}{2}\cdot WW+(A-2B)X_0\cdot t\}+(X_0-t)\{A\cdot QQ+(A-B)2t\}]\frac{\alpha}{2t}$$
$$+[\{\frac{A}{2}\cdot WW+(A-2B)X_0\cdot t\}-(X_0+t)\{A\cdot QQ+(A-B)2t\}]\frac{\beta}{2t},$$

$$u_y = 0,$$

Y-directional linear distributed load

$Y_0\neq 0$

$$\sigma_x = [\{(-m+2n)AA - \frac{m-n}{4}\cdot CC\}\frac{Y_0}{2t} + (\frac{m-3n}{2}\cdot FF + \frac{m-n}{4}\cdot SS)\frac{X_0-t}{2t}]\alpha$$
$$+[-\{(-m+2n)AA - \frac{m-n}{4}\cdot CC\}\frac{Y_0}{2t} - (\frac{m-3n}{2}\cdot FF + \frac{m-n}{4}\cdot SS)\frac{X_0+t}{2t}]\beta,$$

$$\sigma_y = [(-n\cdot AA + \frac{m-n}{4}\cdot CC)\frac{Y_0}{2t} + (\frac{m+n}{2}\cdot FF - \frac{m-n}{4}\cdot SS)\frac{X_0-t}{2t}]\alpha$$
$$+[-(-n\cdot AA + \frac{m-n}{4}\cdot CC)\frac{Y_0}{2t} - (\frac{m+n}{2}\cdot FF - \frac{m-n}{4}\cdot SS)\frac{X_0+t}{2t}]\beta,$$

$$\tau_{xy} = [-(-n\cdot TT + \frac{m-3n}{2}\cdot FF + \frac{m-n}{4}\cdot SS)\frac{Y_0}{2t} + (n\cdot AA - \frac{m-n}{4}\cdot CC)\frac{X_0-t}{2t}]\alpha$$
$$+[(-n\cdot TT + \frac{m-3n}{2}\cdot FF + \frac{m-n}{4}\cdot SS)\frac{Y_0}{2t} - (n\cdot AA - \frac{m-n}{4}\cdot CC)\frac{X_0+t}{2t}]\beta,$$

$$u_x = [-(TT+FF)Y_0 - AA(X_0-t)]B\cdot\frac{Y_0}{2t}\cdot\alpha$$
$$+[(TT+FF)Y_0 + AA(X_0+t)]B\cdot\frac{Y_0}{2t}\cdot\beta,$$

$$u_y = [\{A(\frac{GG}{2}+\frac{HH}{4}) + B\cdot AA\}Y_0 - \{A(EE+TT) + (A+B)FF\}(X_0-t)]\frac{Y_0}{2t}\cdot\alpha$$
$$+[-\{A(\frac{GG}{2}+\frac{HH}{4}) + B\cdot AA\}Y_0 + \{A(EE+TT) + (A+B)FF\}(X_0+t)]\frac{Y_0}{2t}\cdot\beta,$$

$Y_0 = 0$, $|X_0| \fallingdotseq t$

$$\sigma_x = \begin{cases} 0 & (|X_0| > t), \\ -\frac{\nu(X_0-t)}{4t}\cdot\alpha + \frac{\nu(X_0+t)}{4t}\cdot\beta & (|X_0| < t), \end{cases}$$

$$\sigma_y = \begin{cases} 0 & (|X_0| > t), \\ -\frac{(X_0-t)}{4t}\cdot\alpha + \frac{(X_0+t)}{4t}\cdot\beta & (|X_0| < t), \end{cases}$$

$$\tau_{xy} = -n(1+BB\cdot\frac{X_0-t}{2t})\alpha + n(1+BB\cdot\frac{X_0+t}{2t})\beta,$$

$$u_x = 0,$$

$$u_y = [-(\frac{WW}{2} + X_0\cdot t) + (QQ+2t)(X_0-t)]\frac{A}{2t}\cdot\alpha$$
$$+[(\frac{WW}{2} + X_0\cdot t) - (QQ+2t)(X_0+t)]\frac{A}{2t}\cdot\beta,$$

where, $m = \frac{3+\nu}{4\pi}$, $n = \frac{1-\nu}{4\pi}$, $A = \frac{(\nu-3)(\nu+1)}{4\pi E}$, $B = \frac{(\nu+1)(\nu+1)}{4\pi E}$,

$CC = \cos(2\theta_b) - \cos(2\theta_a)$, $SS = \sin(2\theta_b) - \sin(2\theta_a)$, $FF = \theta_b - \theta_a$

$AA = \ln\left|\frac{\sin\theta_b}{\sin\theta_a}\right|$, $TT = \cot\theta_b - \cot\theta_a$,

$$EE = \cot\theta_b \cdot \ln\left|\frac{\sin\theta_b}{Y_0}\right| - \cot\theta_a \cdot \ln\left|\frac{\sin\theta_a}{Y_0}\right|,$$

$$GG = \frac{1}{\sin^2\theta_b} \cdot \ln\left|\frac{\sin\theta_b}{Y_0}\right| - \frac{1}{\sin^2\theta_a} \cdot \ln\left|\frac{\sin\theta_a}{Y_0}\right|,$$

$$HH = \frac{1}{\sin^2\theta_b} - \frac{1}{\sin^2\theta_a}, \quad BB = \ln\left|\frac{X_0 - t}{X_0 + t}\right|,$$

$$QQ = (X_0 - t)\ln|X_0 - t| - (X_0 + t)\ln|X_0 + t|,$$

$$WW = (X_0 - t)^2 \ln|X_0 - t| - (X_0 + t)^2 \ln|X_0 + t|$$

2.4 *Comparison of Solutions*

Figure 4 shows a beam subject to center-point bending. The geometry of the problem and the element discretization of one half of the domain because of symmetry are shown in the

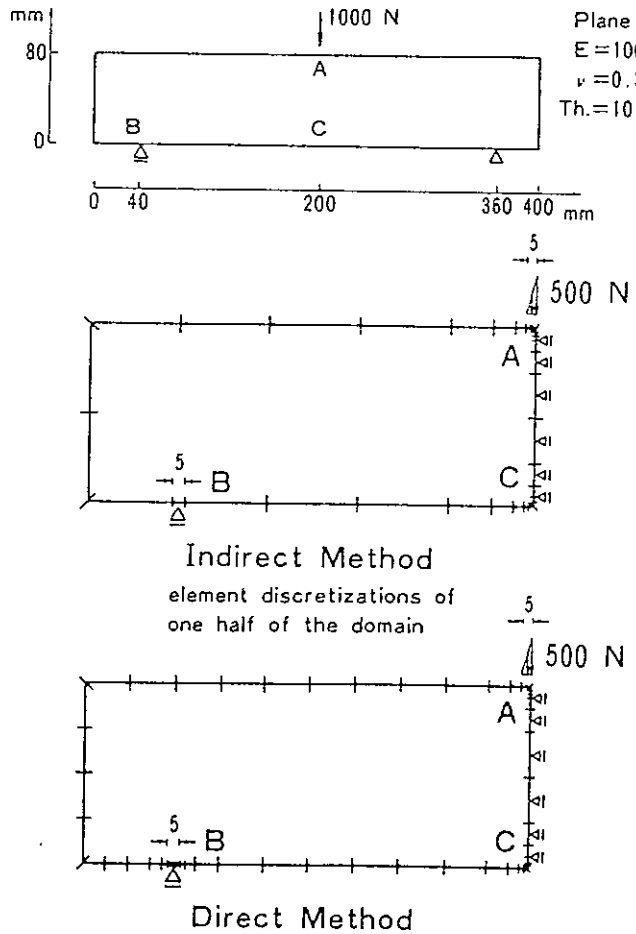

Fig. 4 Beam subject to center-point bending

figure. Figure 5 shows the numerical solutions of unknown boundary values on support B and section AC. The solution by the direct method is the solution of the unknown in the simultaneous algebraic equation composed from Eq. (2). In case of the direct method, the sum of the reacting forces is reasonable, but the distribution is insufficient on the individual elements. However, since the boundary integral of Eq. (4) is calculated along the entire boundary, and the error in the boundary value distribution condition does not affect the stress solutions for the central locations of the individual elements, the stress solutions for the center points of the individual elements on section AC are of comparatively good accuracies.

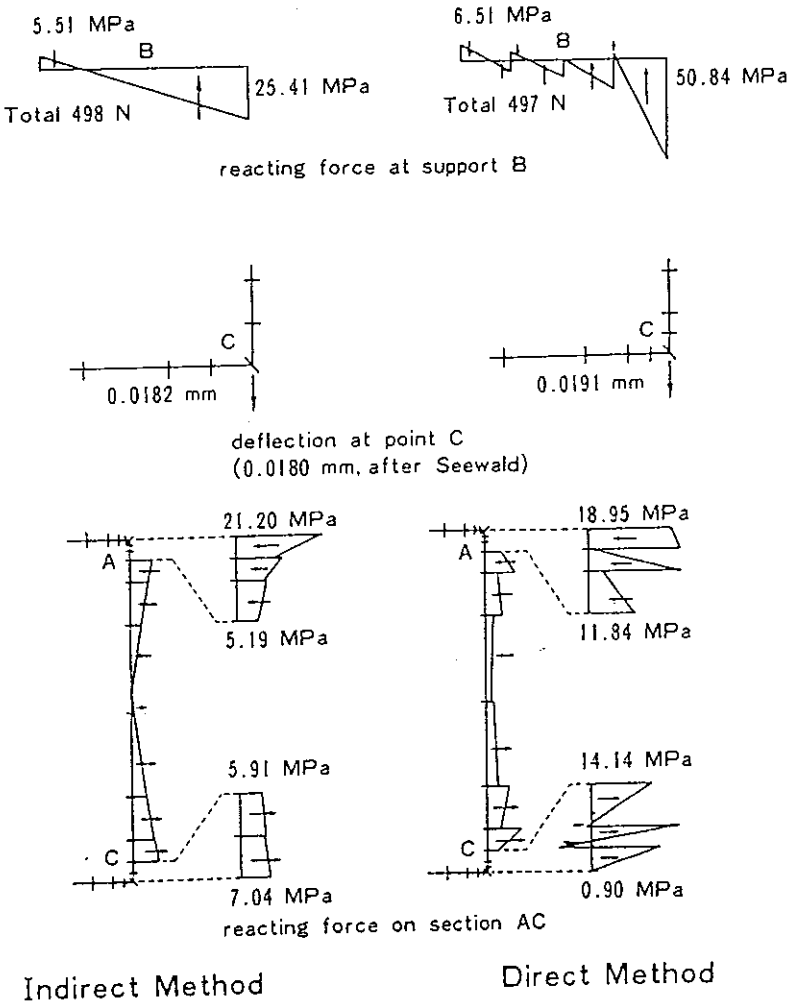

Fig. 5 Comparisons of numerical solutions by the direct and indirect methods

Points A and B in Fig. 4 will need to be handled as singular points. With the direct method, if element discretization in the vicinity of a singular point is roughly made, a large error over the entire domain will be produced in the solution, whereas the indirect method will give a satisfactory solution.

The above are the reasons formulation of the indirect method was selected in this study for J-integral calculation.

3. J-Integral Method

3.1 Formulation of J-Integral Calculation by Indirect Method

Since J-integral is equivalent to the strain energy release rate in relation to a linear elastic body, the stress intensity factor may be tied to the J-integral by the following equation.

$$J=\frac{\kappa+1}{8G}(K_I^2+K_{II}^2)+\frac{1}{2G}K_{III}^2\,, \tag{10}$$

where, J = J-integral

K_I, K_{II}, K_{III} = stress intensity factors for crack opening modes *I, II, III,* respectively

$$\kappa=\begin{cases}(3-\nu)/(1+\nu): \text{plane stress condition}\\ (3-4\nu) \quad : \text{plane strain condition}\end{cases}$$

G = modulus of elasticity in shear

ν = Poisson's ratio

Now, if the coordinate system shown in Fig. 6 is defined and Γ is an arbitrary counter-clockwise path enveloping the crack tip;

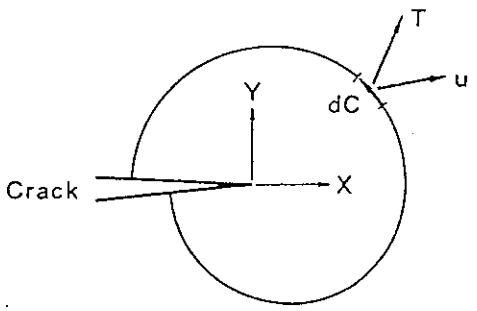

Fig. 6 J-integral

$$J=\oint_{\Gamma}\left\{\omega dY-T_i\cdot\frac{\partial u_i}{\partial X}\,dC\right\}, \tag{11}$$

where, ω = strain energy density

T = distributed force acting from outside along Γ

u = displacement on Γ

dc = line element measured along Γ

If k number of domains in static equilibrium are superposed in order to formulate Eq. (11) by the indirect method, the following equation is obtained.

$$\begin{cases} \omega = \sum^{k} {}^{*st}\omega \cdot W_t^s , \\ T_i = \sum^{k} {}^{*st}T_i \cdot W_t^s , \\ \dfrac{\partial u_i}{\partial X} = \sum^{k} \dfrac{\partial {}^{*st}u_i}{\partial X} \cdot W_t^s , \end{cases} \tag{12}$$

When Eq. (11) is substituted in Eq. (12);

$$J = \oint_{\Gamma} \{ (\sum^{k} {}^{*st}\omega \cdot W_t^s) dY - (\sum^{k} {}^{*st}T_i \cdot W_t^s)(\sum^{k} \frac{\partial {}^{*st}u_i}{\partial X} \cdot W_t^s) dC \} , \tag{13}$$

In order to calculate Eq. (13) numerically, if the path Γ is divided into m number of straight segment elements, the J-integral is determined approximately by the following equation as the total sum of discrete values at the center points of the various path elements.

$$J \fallingdotseq \sum^{m} \{ (\sum^{k} {}^{*st}\omega \cdot W_t^s) \Delta Y - (\sum^{k} {}^{*st}T_i \cdot W_t^s)(\sum^{k} \frac{\partial {}^{*st}u_i}{\partial X} \cdot W_t^s) \Delta C \} , \tag{14}$$

The term $(\sum^{k} \frac{\partial {}^{*st}u_i}{\partial X} \cdot W_t^s)$ in Eq. (14) can be calculated superposing crack-directional differential values of the fundamental solutions. Hence, an analytical formula of partial derivatives of displacements in the fundamental solution shown in Fig. 2 was deduced.

3.2 *Partial Derivatives of Fundamental Solution*

The partial derivatives of displacements produced by linear distributed loads acting in-plane on an infinite plate are shown below in a plane stress condition (see Fig. 3).

X-directional linear distributed load

$Y_0 \neq 0$

$$\frac{\partial u_x}{\partial X} = \{ \{ -A \cdot TT + (B-A) FF + \frac{B}{2} \cdot SS \} Y_0 - (A \cdot AA - \frac{B}{2} \cdot CC)(X_0 - t) \} \frac{\alpha}{2t}$$
$$+ \{ -\{ -A \cdot TT + (B-A) AA + \frac{B}{2} \cdot SS \} Y_0 + (A \cdot AA - \frac{B}{2} \cdot CC)(X_0 + t) \} \frac{\beta}{2t} ,$$

$$\frac{\partial u_x}{\partial Y} = [\{ (A-2B) AA - \frac{B}{2} \cdot CC \} Y_0 - \{ (A-B) FF - \frac{B}{2} \cdot SS \} (X_0 - t)] \frac{\alpha}{2t}$$
$$+ [- \{ (A-2B) AA - \frac{B}{2} \cdot CC \} Y_0 + \{ (A-B) FF - \frac{B}{2} \cdot SS \} (X_0 + t)] \frac{\beta}{2t} ,$$

$$\frac{\partial u_y}{\partial X} = [-B(AA + \frac{CC}{2}) Y_0 + \frac{B}{2} \cdot SS (X_0 - t)] \frac{\alpha}{2t}$$
$$+ [B(AA + \frac{CC}{2}) Y_0 - \frac{B}{2} \cdot SS (X_0 + t)] \frac{\beta}{2t} ,$$

$$\frac{\partial u_y}{\partial Y}=\left[-B\left(TT+\frac{SS}{2}+2FF\right)Y_0-B\left(AA+\frac{CC}{2}\right)(X_0-t)\right]\frac{\alpha}{2t}$$
$$+\left[B\left(TT+\frac{SS}{2}+2FF\right)Y_0+B\left(AA+\frac{CC}{2}\right)(X_0+t)\right]\frac{\beta}{2t},$$

$Y_0=0,\ |X_0|\neq t$

$$\frac{\partial u_x}{\partial X}=A\left(1+BB\cdot\frac{X_0-t}{2t}\right)\alpha-A\left(1+BB\cdot\frac{X_0+t}{2t}\right)\beta,$$

$$\frac{\partial u_x}{\partial Y}=\begin{cases}0 & (|X_0|>t),\\ \pi(A-B)\dfrac{X_0-t}{2t}\cdot\alpha-\pi(A-B)\dfrac{X_0+t}{2t}\cdot\beta & (|X_0|<t),\end{cases}$$

$$\frac{\partial u_y}{\partial X}=0,$$

$$\frac{\partial u_y}{\partial Y}=B\left(1+BB\cdot\frac{X_0-t}{2t}\right)\alpha-B\left(1+BB\cdot\frac{X_0+t}{2t}\right)\beta,$$

Y-directional linear distributed load

$Y_0\neq 0$

$$\frac{\partial u_x}{\partial X}=\left[-B\left(AA+\frac{CC}{2}\right)Y_0+\frac{B}{2}\cdot SS(X_0-t)\right]\frac{\alpha}{2t}$$
$$+\left[B\left(AA+\frac{CC}{2}\right)Y_0-\frac{B}{2}SS(X_0+t)\right]\frac{\beta}{2t},$$

$$\frac{\partial u_x}{\partial Y}=\left[-B\left(TT+\frac{SS}{2}+2FF\right)Y_0-B\left(AA+\frac{CC}{2}\right)(X_0-t)\right]\frac{\alpha}{2t}$$
$$+\left[B\left(TT+\frac{SS}{2}+2FF\right)Y_0+B\left(AA+\frac{CC}{2}\right)(X_0+t)\right]\frac{\beta}{2t},$$

$$\frac{\partial u_y}{\partial X}=\left[-\left\{A\cdot TT+\frac{B}{2}\cdot SS+(A+B)FF\right\}Y_0-\left(A\cdot AA+\frac{B}{2}\cdot CC\right)(X_0-t)\right]\frac{\alpha}{2t}$$
$$+\left[\left\{A\cdot TT+\frac{B}{2}\cdot SS+(A+B)FF\right\}Y_0+\left(A\cdot AA+\frac{B}{2}\cdot CC\right)(X_0+t)\right]\frac{\beta}{2t},$$

$$\frac{\partial u_y}{\partial Y}=\left[\left\{(A+2B)AA+\frac{B}{2}\cdot CC\right\}Y_0-\left\{(A+B)FF+\frac{B}{2}\cdot SS\right\}(X_0-t)\right]\frac{\alpha}{2t}$$
$$+\left[-\left\{(A+2B)AA+\frac{B}{2}\cdot CC\right\}Y_0+\left\{(A+B)FF+\frac{B}{2}\cdot SS\right\}(X_0+t)\right]\frac{\beta}{2t},$$

$Y_0=0,\ |X_0|\neq t$

$$\frac{\partial u_x}{\partial X}=0,$$

$$\frac{\partial u_x}{\partial Y}=B\left(1+BB\cdot\frac{X_0-t}{2t}\right)\alpha-B\left(1+BB\cdot\frac{X_0+t}{2t}\right)\beta,$$

$$\frac{\partial u_y}{\partial X} = A\left(1+BB\cdot\frac{X_0-t}{2t}\right)\alpha - A\left(1+BB\cdot\frac{X_0+t}{2t}\right)\beta ,$$

$$\frac{\partial u_y}{\partial Y} = \begin{cases} 0 & (|X_0|>t) , \\ \pi(A+B)\dfrac{X_0-t}{2t}\cdot\alpha - \pi(A+B)\dfrac{X_0+t}{2t}\cdot\beta & (|X_0|<t) , \end{cases}$$

3.3 *Examples*

In the analyses described below, the stress intensity factor K_I of mode I was calculated in a plane stress condition.

Square plate with central crack under uniform tension

Figure 7 shows the geometry of the problem and element discretizations of a quarter of the domain because of symmetry. The influence of the location of the J-integral path from the

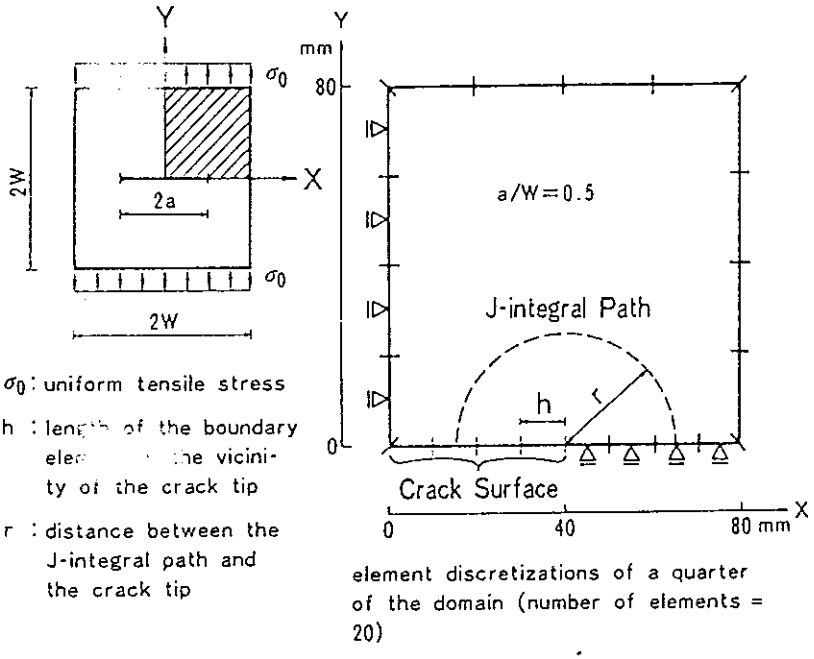

Fig. 7 Square plate with central crack under uniform tension

crack tip on the accuracy of the solution is shown in Fig. 8. If the J-integral path is taken at a location distant from the crack tip by more than h, the length of the boundary element in the vicinity, a stable and accurate solution is obtained regardless of whether the element discretization was fine or coarse. As for the number of path divisions, this does not affect the accuracy of the solution so much except in an exceedingly few cases.

Figure 9 shows comparisons of various crack analysis techniques, where, the energy method is a technique for obtaining the degree of potential energy reduction (strain energy

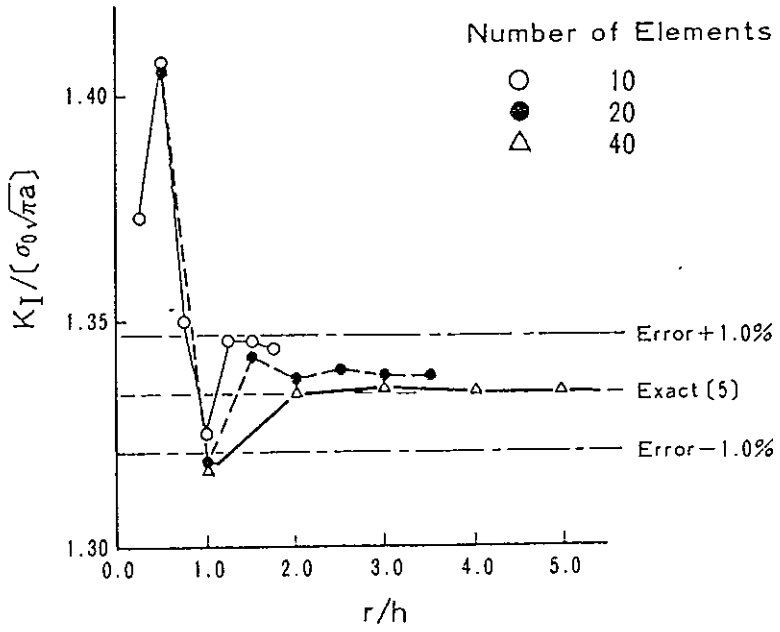

Fig. 8 Influence of the location of the J-integral path from the crack tip on the accuracy of the solution

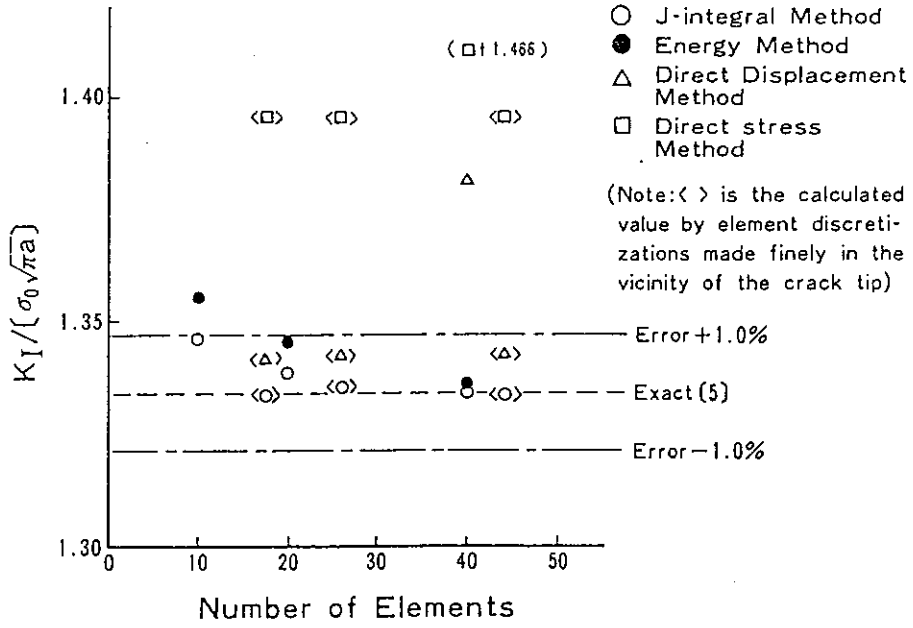

Fig. 9 Comparisons of various crack analysis techniques

release rate) dV/da accompanying crack propagation by differential approximation $\Delta V/\Delta a$, and the direct stress method and direct displacement method are techniques for obtaining stress intensity factors by extrapolation of calculated values of stresses and displacements in the vicinities of crack tips. It may be seen from the figure that the J-integral method is superior in accuracy and economy compared with other techniques.

Rectangular plate with edge crack under uniform tension, pure bending and center-point bending

Figure 10 shows the geometry and boundary conditions of the problem, and element discretizations. Because of symmetry, only half of the domain is shown. The influences of the

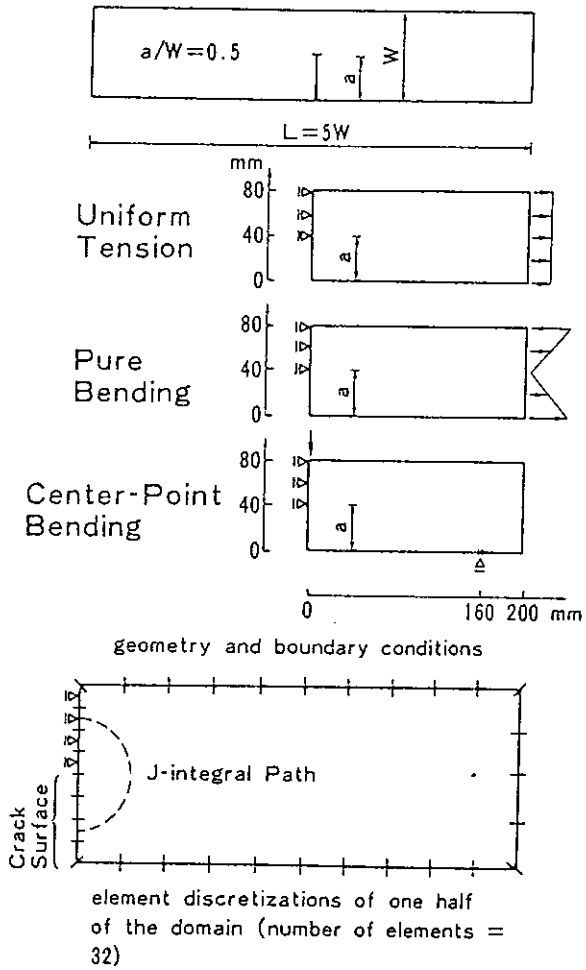

Fig. 10 Rectangular plate with edge crack under uniform tension, pure bending and center-point bending

numbers of element discretizations on solution accuracies are shown in Fig. 11. In case the domain is long and narrow, and is subject to bending as in this type of problem, sufficiently satisfactory accuracies of solutions are obtained for all problems by making element discretizations of the whole narrow to an extent, and also finely dividing crack-tip and corner parts.

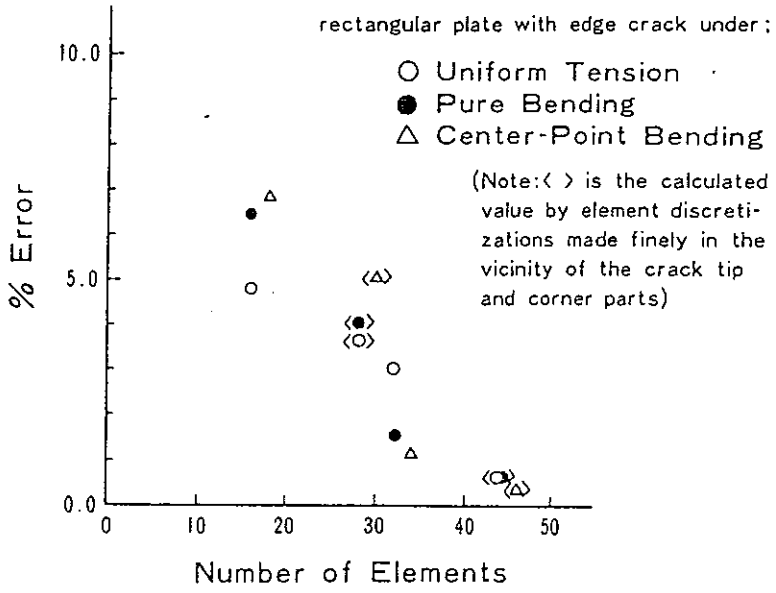

Fig. 11 Influences of the numbers of element discretizations on solution accuracies

Table 2 shows the influences of crack lengths on accuracies of solutions. The results of analyses by this J-integral method on five kinds of crack-length ratios to plate width in the range of 0.1 to 0.5 for the individual problems are shown. The solutions all have errors within 2%, which agrees with exact solutions.

Beam with edge crack subjected to some retraint at supports

The geometry and boundary conditions of the problem are shown in Fig. 12. Four kinds of support restraint conditions were assumed. Restraint of 100% means a restraint condition in which there are no horizontal displacements of supports, while restraints of 66.7% and 33.3% mean restraint conditions of reacting forces of 2/3 H and 1/3 H respectively acting at supports, where H is the size of horizontal reacting force at a support in case of restraint of 100%.

Figure 13 shows stress intensity factors calculated by the present method for various forms of loading in case of restraint of 0%, and Fig. 14 for third-point bending beams subjected to restraint at supports. The variations according to crack lengths and restraint conditions are suitable.

Table 2. Influences of crack lengths on accuracies of solutions

Rectangular plate with edge crack under;	a/W	Exact [5]	Present	% Error
Uniform Tension	0.1	2.11	2.11	+0.0
	0.2	2.43	2.43	+0.0
$Y = K_I / [\sigma_t \sqrt{a}]$	0.3	2.95	2.94	−0.2
	0.4	3.74	3.73	−0.2
(σ_t: tensile stress)	0.5	4.98	4.97	−0.2
Pure Bending	0.1	1.852	1.843	−0.49
	0.2	1.869	1.860	−0.48
$Y = K_I / [\sigma_b \sqrt{a}]$	0.3	1.992	1.977	−0.76
	0.4	2.229	2.209	−0.91
(σ_b: nominal flexural stress)	0.5	2.651	2.610	−1.57
Center-Point Bending	0.1	1.746	1.738	−0.46
	0.2	1.738	1.735	−0.17
$Y = K_I / [\sigma_b \sqrt{a}]$	0.3	1.848	1.840	−0.43
	0.4	2.080	2.064	−0.78
(σ_b: nominal flexural stress)	0.5	2.501	2.471	−1.21

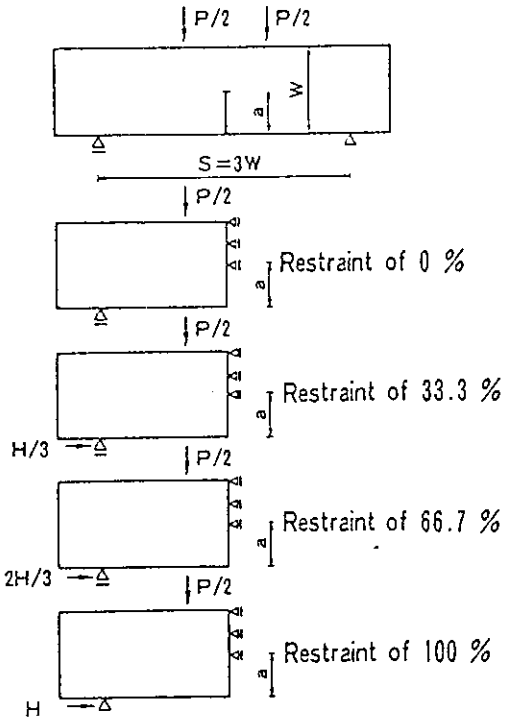

geometry and support restraint conditions

Fig. 12 Beam with edge crack subjected to some restraint at supports

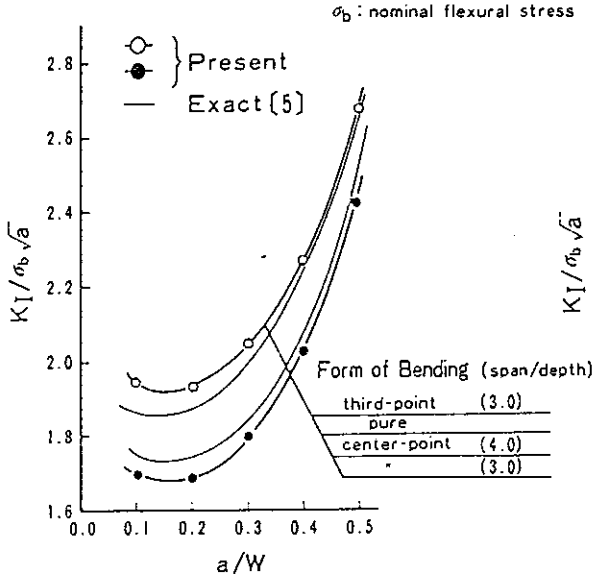

Fig. 13 Variations of stress intensity factor K_I for various forms of loading (in case of restraint of 0%)

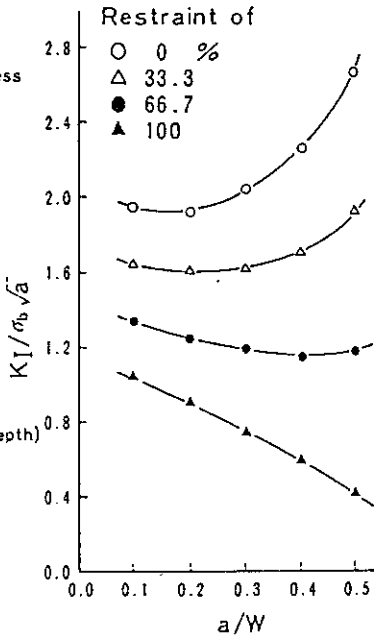

Fig. 14 Variations of stress intensity factor K_I for various support restraint conditions (in case of third-point bending beam)

4. Conclusions

The accuracies of solutions by BEM based on formulation of direct and indirect methods were examined in preliminary studies. As a result, it was indicated that satisfactory solutions are calculated by formulation of the indirect method and not the direct method.

Formulation of J-integral calculation by the indirect method was done and applications were made in analysis of a number of typical crack problems. This J-integral method gives excellent analyzing accuracy in executing problems, and it is thought that a potent means has been provided for calculation of stress intensity factors of cracks encountered in engineering analyses.

References

1) Brebbia, C. A.: *The Boundary Element Method for Engineers*, Pentech Press, London (1980).
2) Hirai, T.: Analytical Formulas for Boundary Integration and Functions Simulating the Distribution of Boundary Values in Boundary Element Method, Proc. Kyushu Branch of Architectural Inst. of Japan, 149 (1983).
3) Hirai, T.: Some Considerations on Indirect and Direct Methods of Boundary Element Method for Two-Dimensional Elasticity Problems, Trans. of Architectural Inst. of Japan, No. 320, 45–55 (1982).
4) Hirai, T.: Some Considerations on Numerical Solutions of Two-Dimensional Elasticity Problems by Superposition of Elementary Solutions, Trans. of Architectural Inst. of Japan, No. 311, 1–10 (1982).

5) Ishida, M.: *Elastic Analysis for Crack and Stress Intensity Factors*, ed. Baihukan, Tokyo (1976).
6) Patterson, C. and Sheikh, M. A.: Regular Boundary Integral Equations for Stress Analysis, Proc. of the Third International Seminar, Irvine, California, 85–104 (1981).
7) Rice, J. R.: Path Independent Integral and the Approximate Analysis of Strain Concentration by Notches and Cracks, J. Apply. Mech., Vol. 35, 379–385 (1968).
8) Seewald, F., p121 in *Theory of Elasticity* by Timoshenko, S. P. and Goodier, J. N., 3rd ed., McGraw-Hill (1927).